Design of Luenberger state observers using fixed-structure H-infinity optimization and its application to fault detection in lane-keeping control of automated vehicles

AUTHOR(S):

Ibaraki, S; Suryanarayanan, S; Tomizuka, M

Design of Luenberger State Observers Using Fixed-Structure $\mathcal{H}_\infty$ Optimization and its Application to Fault Detection in Lane-Keeping Control of Automated Vehicles

Soichi Ibaraki, Shashikanth Suryanarayanan, *Member, IEEE*, and Masayoshi Tomizuka, *Fellow, IEEE*

***Abstract*—Lane-keeping control forms an integral part of fully automated intelligent vehicle highway systems (IVHS) and its reliable operation is critical to the operation of an automated highway. In this paper, we present the design of a fault detection filter for the lane-keeping control systems onboard vehicles used by California-PATH, USA in its automated highways program. We use a Luenberger structure for the fault detection filters and tune the observer gains based on an $\mathcal{H}_\infty$-based cost. Such a choice of cost was motivated by the need to explicitly incorporate frequency-domain-based performance objectives. The linear matrix inequality (LMI)-based formulation of an $\mathcal{H}_\infty$ optimization problem of Luenberger state observers does not allow for the augmentation with dynamic performance weightings in the optimization objective, since it makes the problem a nonconvex optimization problem. We present an algorithm to locally solve the problem of the design of Luenberger state observers using $\mathcal{H}_\infty$ optimization by transforming the problem into an $\mathcal{H}_\infty$ static output feedback controller problem. Experimental results demonstrate the efficacy of the tuning methodology by comparing the fault detection performance of filters that use $\mathcal{H}_\infty$ Luenberger observers versus those that use Kalman filters. Implementation issues of the observers are also discussed.**

***Index Terms*—$\mathcal{H}_\infty$ optimization, fault detection, frequency shaping, integrated vehicle highway systems, state estimation.**

I. Introduction

AUTOMATED highway system (AHS) design has been under investigation over the last couple of decades as part of an effort to develop intelligent and efficient transportation systems for the future. Several research initiatives around the world have focused on AHS development with varying degrees of automation. In the U.S., [1] California PATH has been an active agency working on AHS technology. In 1997, the National Automated Highway System Consortium (NAHSC) conducted a demonstration on the I-15 lanes in San Diego, CA. Demo '97 showcased a prototype of a platoon of fully automated passenger vehicles and, thus, showed that automated highways were a realistic policy option for the future. For a detailed description of the PATH AHS architecture, refer to [1] and [2].

Since 1997, PATH has increased its focus on AHS deployment related issues, such as safety and reliability (see [3] for a comprehensive review of fault-management schemes for automated vehicles in the context of AHS). As part of this overall scheme, several research efforts [4] have focused on fault-management issues for different subsystems of the PATH AHS architecture. The research effort documented in this paper deals with the lane-keeping control system. Since lane-keeping is a critical operation that vehicles in an automated highway need to perform, the reliable operation of the lane-keeping control system is critical to the safe and smooth functioning of the automated highway.

In this paper, we present the design of a fault detection filter for the lane-keeping control system implemented on vehicles used by PATH. The filter design is based on an $\mathcal{H}_\infty$-cost-based methodology for the design of a Luenberger-type state observers. An $\mathcal{H}_\infty$ cost-based design methodology is used because such a formulation allows for explicit incorporation of frequency-based performance weightings. We argue that to lower false alarms and missed detection rates, these fault detection filters need to be designed so that the residuals they generate have appropriate frequency components in different operating conditions (nonfaulty versus faulty). We compare the performance of filters designed based on this approach to that of a Kalman filter (which uses an $\mathcal{H}_2$ cost).

Nagpal and Khargonekar [5] showed that the $\mathcal{H}_\infty$ optimization problem of Luenberger state observers with static performance could be, analogous to the case of the Kalman filter, reparameterized as a problem to solve a set of algebraic Ricatti equations (AREs). However, the Luenberger state observer optimization problem with dynamic performance weights cannot be parameterized using AREs, or equivalently, using linear matrix inequalities (LMIs). This paper presents an extension of the $\mathcal{H}_\infty$ optimization algorithm of Luenberger state observers to more general problems with dynamic weightings. The development is analogous to the extension of the $\mathcal{H}_\infty$ optimization of full-order controllers to fixed-order, fixed-structure controllers [6].

Manuscript received May 12, 2003; revised December 30, 2003. This work was supported in part by the California Department of Transportation (CalTrans) under PATH MOU 373.

S. Ibaraki is with the Department of Precision Engineering, Kyoto University, Kyoto 606-8501, Japan (e-mail: ibaraki@prec.kyoto-u.ac.jp).

S. Suryanarayanan is with the Department of Mechanical Engineering, Indian Institute of Technology Bombay, Mumbai 400076, India (e-mail: shashisn@iitb.ac.in).

M. Tomizuka is with the University of California at Berkeley, Berkeley, CA 94720-1740 USA (e-mail: tomizuka@me.berkeley.edu).

Digital Object Identifier 10.1109/TMECH.2004.842243

[1]Partners for Advanced Transit (PATH), California, is a consortium aimed at using advanced technologies for transit needs http://www.path.berkeley.edu

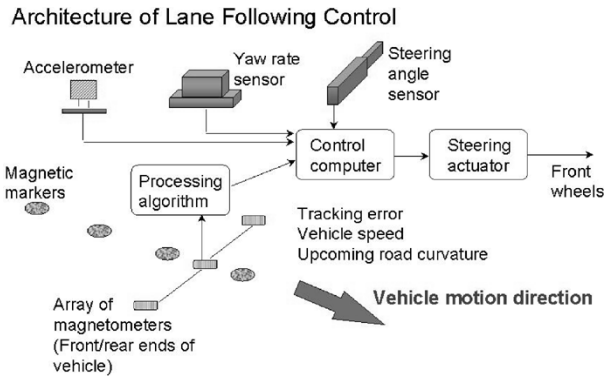

Fig. 1. PATH AHS: Lateral control system hardware.

The paper is organized as follows. Section II details the lateral control system onboard vehicles used by PATH and the structure of the fault detection scheme used for the lane-keeping control system. Section III proposes an algorithm to solve an $\mathcal{H}_\infty$ optimization problem of Luenberger state observers with dynamic weightings. Section IV details the specifics of the application of the method developed in Section III to the fault detection filter design problem. Section V presents experimental results that corroborate the analytical predictions of the design. Section VI discusses the conclusions drawn from the paper and future research.

II. Fault Detection and Identification in the Lane-Keeping Control System of the PATH AHS

A. Lateral Control Hardware Onboard PATH's Vehicles

Fig. 1 shows the schematic of the lateral control hardware installed on test vehicles used by PATH. A magnet-magnetometer-based system is used to realize lane-keeping. Magnets are laid out along the center of lanes. The lane-keeping control problem then boils down to ensuring that vehicles follow the series of magnets. The vehicles, in turn, have a set of sensors (referred to as "magnetometers" in the rest of the paper) that measure the lateral deviation of their location with respect to the magnets (road center-line). The lateral error information is processed by an onboard computer to generate the steering angle required to follow the road center-line. PATH's passenger vehicle hardware architecture consists of two sets of magnetometers mounted under the front and rear bumpers of the vehicle. Each magnetometer set consists of three magnetometers (Three magnetometers are used to increase the range of measurement to about 0.5 m. The other sensors shown in Fig. 1 are used for lane-changing and other purposes).

B. Fault Detection and Identification in the Lane-Keeping Control System of the PATH AHS

A fault is an anomaly that occurs during system operation that can significantly impact performance or stability of the system under operation. Fault detection and identification (FDI) problems in dynamic systems have been an active research area in recent years (see, for example, [7] and [8]). In particular, this paper focuses on the state estimator design frequently encountered in model-based fault detection and identification schemes (e.g., [9]). Model-based FDI schemes utilize the principle of analytical redundancy. The principle can roughly be stated as follows: Assuming that the overall process model "mostly" agrees with the actual process dynamics, faults that change the process behavior will lead to a mismatch ("residuals") between estimated and measured signals. If this mismatch exceeds a prescribed threshold value, it is understood that a fault has occurred.

The application of frequency-domain approaches to fault detection filter design was initiated by Viswanadham *et al.* [10]. They proposed a simple form for constructing the residual generator and suggested the application of $\mathcal{H}_\infty$ optimization to FDI problems. Frank and Ding [11] formulated the FDI problem in a more systematic manner and presented the $\mathcal{H}_\infty$ optimization algorithm to solve it by using factorization techniques.

Since 1997, PATH has increased its focus on deployment related issues, such as safety and reliability. Rajamani *et al.* [4] developed a complete fault diagnostic system structure for automated passenger vehicles to detect all possible faults in 12 sensors and three actuators (e.g., wheel speed sensor, radar range sensor, longitudinal accelerometer, throttle angle sensor, magnetometers; brake actuator, steering actuator, and throttle actuator) used in lateral and longitudinal control systems of the vehicle. The fault diagnostic system monitors all sensor outputs and actuators. A bank of state observers, each of which is based on different combinations of sensor measurements, generates residuals to detect and isolate each possible fault.

In this paper, we focus on a fault detection scheme to detect failures in sensors used for lane-keeping control action, namely, the magnetometers. Note that this approach can be applied to the tuning of other fault detection filters that use observer-based structures.

C. Description of Failures in the Magnetometers

The magnetometers come with a built-in hardware failure detection system that detect a certain set of component failures related to the hardware components of the magnetometers. The magnetometers have a health signal to indicate the condition of operation of the magnetometers. In the event of a hardware failure that can be detected by the magnetometer, the magnetometer output is set to maximum.

However, two other failure conditions have been found to occur in practice. The first relates to sensor disconnection usually caused due to physical damage to the magnetometers. Such situations have occurred mainly during operation of the vehicles under harsh environmental conditions (e.g., on an automated snow-plow machine or during operation under heavy rains). This fault is very severe and causes stability problems [12], [13] though it is fairly easy to detect.

The other conditions relates to a drift in the magnetometer output. Drift is not uncommon in analog measuring equipment. From experience with the magnetometers, a reasonable model for the drift is an offset in the measured value of the magnetometer output. This anomaly/failure is difficult to detect. In this paper, we focus on the detection of this failure.

Furthermore, faults are assumed not to occur in both magnetometers simultaneously.

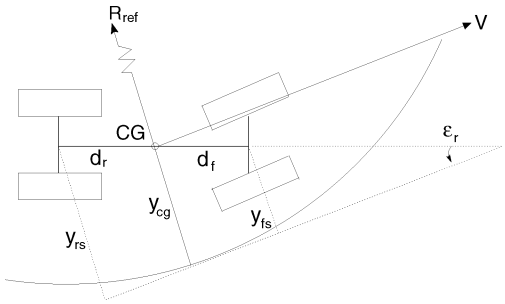

Fig. 2. Four-wheel vehicle following a reference path.

TABLE I
PARAMETERS USED IN THE BICYCLE MODEL

Param.	Description	Values
m	Mass of the vehicle	1700-2100 kg
I_z	Yaw moment of inertia	$\approx$ 2870 kg m^2
l_f	CG-front axle dist.	0.9 - 1.2 m
l_r	CG-rear axle dist	1.5 - 1.8 m
C_f	Cor. stiff. - Front tire	$\approx$ 70000 N/rad
C_r	Cor. stiff. - Rear tire	$\approx$ 130000 N/rad
$\dot{x}$	Forward vel. of vehicle	0- 35 m/s
d_s	Dist. of sensor from CG	-3 to 10 m

D. Bicycle Model for Lateral Control

The design of fault detection filters is based on a simple-yet-powerful model describing the lateral dynamics of a front-wheeled steered vehicle (e.g., [14]). Fig. 2 shows a front-wheel steered vehicle model on a curve of radius R_{ref}.

The "bicycle model" neglects the roll-and-pitch motions in the vehicle and assumes that the relative yaw angle ϵ_r is maintained small. Under these assumptions and treating the longitudinal velocity v as a varying parameter, the lateral motion of the vehicle can be represented by the following linearized model:

$$\begin{aligned} \dot{x} &= Ax + B_1\delta + B_2\dot{\epsilon}_d \\ \begin{bmatrix} y_{fs} \\ y_{rs} \end{bmatrix} &= \begin{bmatrix} 1 & 0 & d_1 & 0 \\ 1 & 0 & -d_2 & 0 \end{bmatrix} x =: Cx \end{aligned} \tag{1}$$

where $x = [\, y_{cg} \quad \dot{y}_{cg} \quad \epsilon_r \quad \dot{\epsilon}_r \,]^T$ is the state variable vector, y_{cg} is the lateral displacement of the vehicle's center of gravity (CG) relative to the road centerline, and ϵ_r is the yaw angle of the vehicle relative to the road centerline (Fig. 2). δ is the steering angle (control input). $\dot{\epsilon}_d$ is the yaw rate associated with road curvature. See the Appendix and Table I for a more detailed description of the system matrices $A \in \mathbb{R}^{4\times4}$ and $B_1, B_2 \in \mathbb{R}^{4\times1}$. y_{fs} and y_{rs} are lateral errors measured by magnetometers installed underneath the front bumper and the rear bumpers, respectively. d_1, d_2 represent the distances between the center-of-gravity and the location of the front and rear magnetometers, respectively.

A single input, single output (SISO) linear controller was implemented for lateral control of the vehicle in lane-following maneuvers. The input to the controller can be interpreted as a frequency-shaped linear combination of the outputs of the magnetometers

$$y_s(s) = \frac{d_2 + d_s(s)}{d_1 + d_2} y_{fs}(s) + \frac{d_1 - d_s(s)}{d_1 + d_2} y_{rs}(s) \tag{2}$$

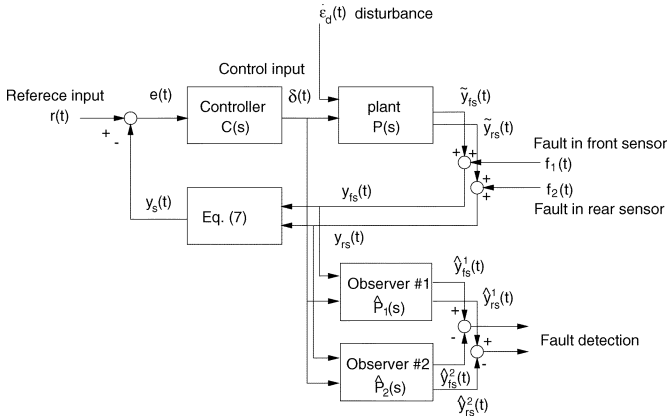

Fig. 3. Fault detection scheme based on dedicated observers.

where $d_s(s)$ is shaped over frequency and can be arbitrarily specified. Notice that y_s represents the lateral error at the location of the virtual sensor, which is at a distance d_s ahead of the vehicle's center-of-gravity [15]. The controller $C(s)$ is essentially given as the combination of a second-order linear lead-lag filter and a notch filter (to account for roll-yaw coupling). It was successfully implemented on a test vehicle and its control performance was verified in simulation and experimentation. For details on the lateral control problem and implementation details, refer to [2] and [15]. The closed-loop configuration of the entire lateral control system is depicted in Fig. 3.

E. Fault Detection Scheme

Fig. 3 also shows the architecture of the fault detection scheme. The dedicated state observer #1 $\hat{P}_1(s)$ estimates the lateral errors at the locations of the front and rear magnetometers by using measured y_{fs} and the steering angle δ. Denote its estimates by $\hat{y}^1_{fs}$ and $\hat{y}^1_{rs}$. The dedicated state observer #2, $\hat{P}_2(s)$ estimates the same two variables based on measured y_{rs} and δ. Denote its estimates by $\hat{y}^2_{fs}$ and $\hat{y}^2_{rs}$. The basic idea of the dedicated observer-based fault detection scheme is as follows. Suppose that a fault occurred in the front sensor. Then, the dedicated observer #1 can no longer estimate the correct lateral errors since it is based on faulty sensor measurement, while the observer #2 is not affected by this fault. Therefore, by monitoring the difference of each observer's estimates, one can detect the fault.

The requirement of any fault detection system is to minimize: 1) missed detections and 2) false alarms in the presence of external disturbances and model uncertainties. In particular, the most significant disturbance to the lateral dynamics of the vehicle is the centripetal acceleration (which acts mostly as a static disturbance) at curved sections of roads. To minimize false alarms, we require that the two dedicated observers $\hat{P}_1(s)$ and $\hat{P}_2(s)$ are designed such that the differences of their estimates $\hat{y}^1_{fs} - \hat{y}^2_{fs}$ and $\hat{y}^1_{rs} - \hat{y}^2_{rs}$ are kept small (compared to a designed threshold value) during nonfaulty operations (so that faults can be distinguished from disturbances). Also, steady-state gains from the disturbance to the estimates under no-fault conditions need to be maintained small.

As a motivation for utilizing the dedicated observer-based architecture, we note that Suryanarayanan and Tomizuka [13]

proposed a fault-tolerant controller for lateral control of automated passenger vehicles, which guarantees the stability of the closed-loop system under failures (as described earlier). This fault tolerant scheme is based on a dedicated state observer-based architecture, identical to the one shown in Fig. 3. Therefore, the fault detection scheme presented in this section can be implemented without making any significant changes to the fault-tolerant control architecture (We wish to add here that by a fault-tolerant controller, we mean a controller that is robust to failures in magnetometers.).

III. Frequency-Domain Design of State Observers by Fixed-Structure $\mathcal{H}_\infty$ Optimization

In this paper, we demonstrate a frequency-shaping design of the dedicated observers $\hat{P}_1(s)$ and $\hat{P}_2(s)$ in Fig. 3 by using the fixed-structure $\mathcal{H}_\infty$ optimization. First, in this section, we show that an $\mathcal{H}_\infty$ optimization problem of a Luenberger state observer can be seen as an extension of a static output feedback $\mathcal{H}_\infty$ controller optimization problem. Therefore, a linearization-based local search algorithm for the reduced-order $\mathcal{H}_\infty$ controller synthesis problem can be straightforwardly applied to this problem.

An $\mathcal{H}_\infty$ optimization problem of Luenberger state observers is formulated as follows. Consider a linear time invariant (LTI) system described using state-space representation by

$$\begin{aligned} \dot{x}(t) &= Ax(t) + Bu(t) + B_w w(t) \\ y(t) &= Cx(t) + D_w w(t) \end{aligned} \tag{3}$$

where $x(t) \in \mathcal{R}^n$ is the state vector, $u(t) \in \mathcal{R}^{m_1}$ is the control input, $y(t) \in \mathcal{R}^{p_1}$ is the measured output, $w(t) \in \mathcal{R}^{m_2}$ denotes a vector containing both the noise and external disturbances with known power spectral densities, and $\hat{x}(t) \in \mathcal{R}^n$ is the estimated state vector. Consider a state observer of the Luenberger observer structure

$$\dot{\hat{x}}(t) = A\hat{x}(t) + Bu(t) + L(y(t) - C\hat{x}(t)). \tag{4}$$

Note that the matrices associated with the estimator are the same as those of the plant. The problem is to tune the estimator gain matrix $L \in \mathcal{R}^{n \times p_1}$ such that $\mathcal{H}_\infty$ norm of the transfer function matrix from the external disturbance $w(t)$ to the weighted state estimation error $z(t)$ (denoted as $T_{w \to z}(s)$) is minimized. $z(t)$ is defined in the s-domain as follows:

$$z(s) = W_p(s)(x(s) - \hat{x}(s)) \tag{5}$$

where $W_p(s)$ is a $p_2 \times n$ weighting transfer function matrix.

When the weighting matrix $W_p(s)$ is a static matrix (i.e., $W_p(s) = W_p \in \mathcal{R}^{p_2 \times n}$), the $\mathcal{H}_\infty$ problem of the observer matrix L can be reparameterized as an LMI problem, or equivalently, a problem to solve a set of AREs as shown by Nagpal and Khargonekar [5]. However, when a dynamic weighting matrix $W_p(s)$ is augmented, it can be easily seen that this problem cannot be rewritten as an LMI problem. This is because when dynamic weights are augmented, the state observer $\hat{P}(s)$ is no longer a full state estimator since the state variables of dynamic weights are not estimated (they do not exist in the physical system). Notice that the analogous observation applies to the $\mathcal{H}_\infty$ synthesis problem of state feedback controllers [16], [17].

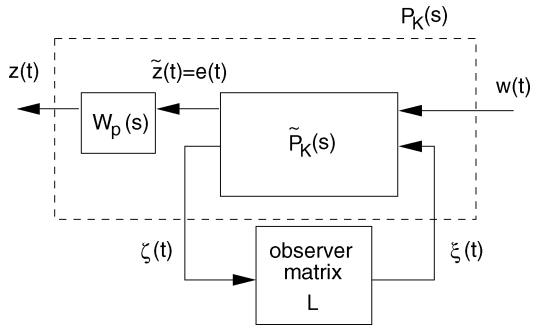

Fig. 4. Extraction of the observer matrix L.

We apply the $\mathcal{H}_\infty$ optimization algorithm for fixed-structure controllers presented by Ibaraki and Tomizuka [18] to locally solve this problem. The algorithm proposed in [18] first transforms an $\mathcal{H}_\infty$ optimization problem of fixed-structure controllers into a synthesis problem of a static output feedback controller by "extracting" tunable controller parameters using linear fractional transformations (LFTs). To illustrate the transformation, first consider the transfer function from $w(t)$ to the state estimation error vector $e(t) := x(t) - \hat{x}(t)$ without a dynamic weighting matrix $W_p(s)$. By combining the plant dynamics (3) and the observer dynamics (4), the state estimation error dynamics is given as follows:

$$\dot{e}(t) = (A - LC)e(t) + B_w w(t). \tag{6}$$

Then, construct the extended plant model $\tilde{P}_K(s)$ as follows (Fig. 4):

$$\begin{aligned} \dot{e}(t) &= Ae(t) + B_w w(t) - \xi(t) \\ \tilde{z}(t) &= e(t) \\ \zeta(t) &= Ce(t). \end{aligned} \tag{7}$$

It is easy to see that $F_L(\tilde{P}_K(s), L)$ is equal to the state estimation error dynamics $T_{w \to e}(s)$, where $F_L(\tilde{P}_K(s), L)$ denotes the closed-loop transfer function from $w(t)$ to $\tilde{z}(t)$ in Fig. 4 (where $\xi(t) = L\zeta(t)$). When a dynamic weighting matrix $W_p(s)$ is augmented, let $P_K(s)$ be the serial combination of $\tilde{P}_K(s)$ and $W_P(s)$, as shown in Fig. 4. Then, $F_L(P_K(s), L)$ becomes equal to the transfer function from $w(t)$ to $z(t)$.

Notice that the observer matrix L is a constant full-block matrix whose entries are all independently tunable. Therefore, the H_∞ optimization problem of the observer matrix L can be seen as an H_∞ synthesis problem of a static output feedback controller for the extended plant model $\mathrm{P}_K(\mathrm{s})$.

Unlike the full-order controller synthesis case, $\mathcal{H}_\infty$ optimization of static (or more generally, reduced-order) output feedback controllers cannot be reparameterized as a convex optimization problem. Several local search algorithms have been proposed to solve this problem. In this paper, we employ the cone complementarity linearization algorithm proposed by El Ghaoui *et al.* [6]. The cone complementarity linearization algorithm is a local search algorithm and, thus, there is no guarantee that it finds the global minimum. However, in most practical applications, it performs excellently, as shown in [6] with extensive numerical examples.

It should be noted that nonconvex $\mathcal{H}_\infty$ optimization problems of state observers have attracted more attention in recent years, mainly from the interest in the design of robust filters (e.g., [19]–[21]). The approach proposed in this paper does not explicitly deal with the robustness issue. We focus on a rather simple application of the $\mathcal{H}_\infty$ optimization to the frequency-domain loop-shaping of state observers. The next section illustrates such an application of the $\mathcal{H}_\infty$ optimization that incorporates the designer's expertise and understanding of a problem and design objectives into the observer design procedure.

IV. Design of Dedicated Observers for Lateral Control of Automated Vehicles

The dedicated state observers $\hat{P}_1(s)$ and $\hat{P}_2(s)$ have the following (Luenberger-type) structure:

$$\begin{aligned}\hat{P}_1(s): \quad \dot{\hat{x}}_1 &= A\hat{x}_1 + B_1\delta + L_1(y_{fs} - \hat{y}^1_{fs}) \\ \begin{bmatrix}\hat{y}^1_{fs} \\ \hat{y}^1_{rs}\end{bmatrix} &= C\hat{x}_1 \\ \hat{P}_2(s): \quad \dot{\hat{x}}_2 &= A\hat{x}_2 + B_1\delta + L_2(y_{rs} - \hat{y}^2_{rs}) \\ \begin{bmatrix}\hat{y}^2_{fs} \\ \hat{y}^2_{rs}\end{bmatrix} &= C\hat{x}_2 \end{aligned} \tag{8}$$

where $\hat{x}_1 \in \mathcal{R}^4$ and $\hat{x}_2 \in \mathcal{R}^4$ are state variables of $\hat{P}_1(s)$ and $\hat{P}_2(s)$. The observer system matrices (A, B_1, C) are the same as those of the plant model given in (1).

A. Inadequacies of Nonfrequency-Shaped Estimator

First, the observer matrices L_1 and L_2 were obtained by using the Kalman filter design, as demonstrated in [13]. Note that the Kalman filter assumes knowledge of power spectral densities and does not lend itself naturally to incorporate frequency shaping. Denote these Kalman filters as $\hat{P}_1^{\rm old}(s)$ and $\hat{P}_2^{\rm old}(s)$.

When $\hat{P}_1^{\rm old}(s)$ and $\hat{P}_2^{\rm old}(s)$ are used, frequency responses of estimation error dynamics from the external disturbance $\dot{\epsilon}_d$ to the estimation error $e_{fs} := y_{fs} - \hat{y}_{fs}$ and $e_{rs} := y_{rs} - \hat{y}_{rs}$ are given, as shown in Fig. 5 (dashed lines). Denote these transfer functions by $T_{\dot{\epsilon}_d \to e_{fs}}(s)$ and $T_{\dot{\epsilon}_d \to e_{rs}}(s)$, respectively.

The figure implies that $\hat{P}_1^{\rm old}(s)$ and $\hat{P}_2^{\rm old}(s)$ are not effective for the purpose of fault detection for the following reasons.

1) The differences of steady-state gains of $\hat{P}_1^{\rm old}(s)$ and $\hat{P}_2^{\rm old}(s)$ are not sufficiently small, especially that in the $T_{\dot{\epsilon}_d \to e_{fs}}(s)$ dynamics.
2) The steady-state gains of error dynamics are not sufficiently small, especially that of $\hat{P}_2^{\rm old}(s)$ in the $T_{\dot{\epsilon}_d \to e_{fs}}(s)$ dynamics.

B. Design of $\hat{P}_2(s)$

It is easy to see that the problem to optimize L_1 and L_2 at the same time cannot be transformed into a static output feedback synthesis problem, as shown in Section III. Therefore, L_1 and L_2 must be optimized in an alternating manner to obtain a locally optimal solution, similarly as shown in [22] for fixed-structure controller optimization cases.

First, consider the tuning problem of L_2, with L_1 fixed to the Kalman filter gain obtained above. The objective is to reduce the gain of estimation error dynamics especially at lower frequencies, without sacrificing the estimation stability. This problem can be cast as an $\mathcal{H}_\infty$ optimization problem as follows:

$$\min_{L_2} \left\| \begin{matrix} W_{p1}(s) T^2_{\dot{\epsilon}_d \to e_{fs}}(s) \\ W_{p2}(s) T^2_{\dot{\epsilon}_d \to e_{rs}}(s) \end{matrix} \right\|_\infty \tag{9}$$

where $T^2_{\dot{\epsilon}_d \to e_{fs}}(s)$ and $T^2_{\dot{\epsilon}_d \to e_{rs}}(s)$ denote the estimation error dynamics of the dedicated observer #2 $\hat{P}_2(s)$. $W_{p1}(s)$ and $W_{p2}(s)$ are dynamic performance weightings, which specify the desired shapes of $|T^2_{\dot{\epsilon}_d \to e_{fs}}(j\omega)|$ and $|T^2_{\dot{\epsilon}_d \to e_{rs}}(j\omega)|$, respectively. $W_{p1}(s)$ and $W_{p2}(s)$ are designed based on actual frequency responses of $T^2_{\dot{\epsilon}_d \to e_{fs}}(s)$ and $T^2_{\dot{\epsilon}_d \to e_{rs}}(s)$ when the Kalman filter $\hat{P}_2^{\rm old}(s)$, is used. This ensures that for this application, the solution of problem (9) achieves better performance than the Kalman filter.

An analogous "loop-shaping" technique to design performance filters in the optimization setting is widely used in the $\mathcal{H}_\infty$ controller design [18]. The numerical values used for W_{p1} and W_{p2} are shown in the Appendix. All computations to solve problem (9) have been carried out on MATLAB by using the LMI Control Toolbox [23]. The (sub)optimal solution, denoted by $\hat{P}_2^{\rm new}(s)$, achieves the $\mathcal{H}_\infty$ norm (9) of 1.425, while $\hat{P}_2^{\rm old}(s)$ gives 15.91. Fig. 5 compares the frequency responses of estimation error dynamics of $\hat{P}_2^{\rm old}(s)$ and $\hat{P}_2^{\rm new}(s)$. The gain reduction at lower frequencies can be clearly observed in both error dynamics.

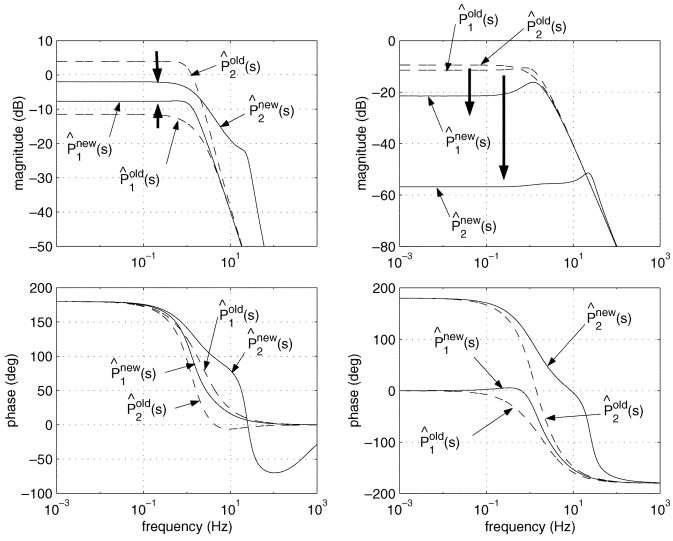

Fig. 5. Comparison of estimation error dynamics of the Kalman filters $P_1^{\rm old}(s)$ and $P_2^{\rm old}(s)$, and the retuned settings $P_1^{\rm new}(s)$ and $P_2^{\rm new}(s)$. (a) Estimation error dynamics of y_{fs}, $|T_{\dot{\epsilon}_d \to e_{fs}}(j\omega)|$. (b) Estimation error dynamics of y_{rs}, $|T_{\dot{\epsilon}_d \to e_{rs}}(j\omega)|$.

C. Design of $\hat{P}_1(s)$

Now, consider the tuning problem of L_1, with L_2 fixed to the value obtained above. The requirement that the detection scheme yields small differences between the estimates of the dedicated observers during nonfaulty operation is translated into the following problem:

$$\min_{L_1} \left\| \begin{matrix} W_{p1}(s)(T^1_{\dot{\epsilon}_d \to e_{fs}}(s) - T^2_{\dot{\epsilon}_d \to e_{fs}}(s)) \\ W_{p2}(s)(T^1_{\dot{\epsilon}_d \to e_{rs}}(s) - T^2_{\dot{\epsilon}_d \to e_{rs}}(s)) \end{matrix} \right\|_\infty \tag{10}$$

where $T^1_{\dot{e}_d \to e_{fs}}(s)$ and $T^1_{\dot{e}_d \to e_{rs}}(s)$ denote the estimation error dynamics of the dedicated observer #1 $\hat{P}_1(s)$. In this problem, the performance weightings $W_{p1}(s)$ and $W_{p2}(s)$ are set to $W_{p1}(s) = W_{p2}(s) = 1$.

Since $\hat{P}_2(s)$ is fixed, problem (10) can also be transformed to an $\mathcal{H}_\infty$ optimization problem of a static outputfeedback gain matrix. The overall plant model in problem (10) is eighth order. Problem (10) was locally solved in the similar manner as the previous case. The (sub)optimal solution, denoted by $\hat{P}_1^{\text{new}}(s)$, achieves the $\mathcal{H}_\infty$ norm (10) of 0.400, while $\hat{P}_1^{\text{old}}(s)$ gives 0.626. Since no significant improvement was achieved by further iterations, the design procedure was terminated at this point.

D. Comparisons Between the Kalman Filter and $\mathcal{H}_\infty$-Based Observers

Fig. 5 compares estimation error dynamics of the Kalman filters $\hat{P}_1^{\text{old}}(s)$ and $\hat{P}_2^{\text{old}}(s)$ (dashed lines), and the retuned observers $\hat{P}_1^{\text{new}}(s)$ and $\hat{P}_2^{\text{new}}(s)$ (solid lines). In Fig. 5(a), it can be observed that the steady-state error of $\hat{P}_2(s)$ was reduced by the tuning, while that of $\hat{P}_1(s)$ was slightly increased to reduce the gap between two observers. Fig. 5(b) shows that the steady-state errors of two observers were both significantly reduced and, therefore, the difference of steady-state errors was also reduced.

It should be noted that the detection scheme utilized in this paper cannot isolate the failures (i.e., we have not focused on how to differentiate failure in the rear magnetometer from a similar failure with the front set of magnetometers). There are methods to do this, which is not the focus of the paper. The paper intends to focus on failure detection and how it fits into the scheme of design of frequency-shaped observers.

V. Experimental and Emulation Results

This section presents two sets of results comparing the performance of the $\mathcal{H}_\infty$ optimization-based observers versus that of the Kalman filters. The first set of results relate to low-speed experimental results. Experiments were conducted on passenger test vehicles used by PATH (Buick LeSabres). High-speed experimental testing has not been conducted yet. However, the efficacy of the proposed scheme has been tested in emulation (i.e., real data from previous high-speed tests have been used as observer inputs).

A. Low-Speed Experimental Results

Low-speed (< 30 mph) tests were conducted on PATH's Richmond Field Station test track in Richmond, CA. The test track consists of several sharp curves.

To compare the failure detection performance of the Kalman filter-based dedicated observer scheme versus the $\mathcal{H}_\infty$ optimized dedicated observer scheme, four observers (two each for the Kalman filter and the $\mathcal{H}_\infty$ optimized observers) were run in parallel in real time. The difference between the estimates based of the front and rear magnetometer measurements was compared for the two fault detection schemes (one based on Kalman filters and the other based on $\mathcal{H}_\infty$ optimized Luenberger observers).

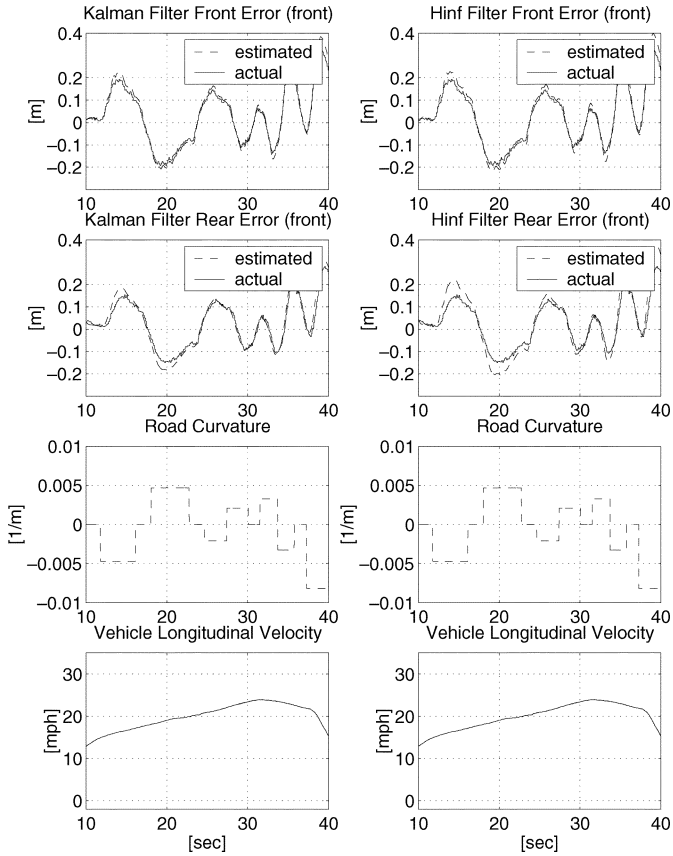

Fig. 6. Comparison of estimation performance of dedicated observer based only on the front magnetometer measurement (low speed).

Fig. 6 shows how the estimation performance of the $\mathcal{H}_\infty$ optimized Luenberger observer compares with that of the Kalman filter at low speeds. Both the Kalman filter and the $\mathcal{H}_\infty$ optimized observer shown here are dedicated observers based on the front magnetometer measurement alone. The performance comparisons for the rear magnetometer-based observers exhibit a similar character (we have omitted related plots in the interest of brevity). The longitudinal velocity of the vehicle was set to 25 mph for the design of the observers. It can be seen that the observers estimate the variables precisely.

Fig. 7 shows the evolution of the difference between estimates (for the front lateral error) from the two dedicated observers. An offset fault (corresponding to drift, refer to Section II-C) is emulated at $\mathrm{t} = 15$ s. Note that all of the estimates are filtered by a low-pass filter. We observe that the difference between estimates deviates away from its no-fault value. It can be seen that, however, when Kalman filters are used, we *cannot* distinguish between a fault in the rear magnetometer from the no-fault operation case. This is because the difference between estimates under no-fault Kalman filter-based operation is not small enough.

B. High-Speed Test Emulation

Real-time testing of the performance of observers at high speeds has not been performed so far. However, we have carried out emulation studies based on experimental data obtained from previous tests conducted at high speeds.

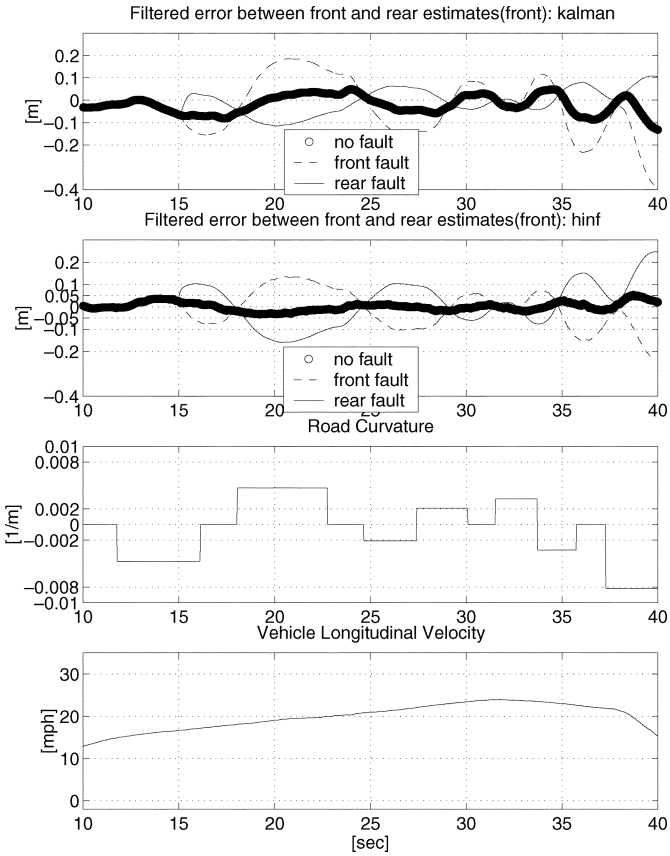

Fig. 7. Comparison of the difference between estimates of dedicated observers based only on the front magnetometer measurement (filtered, low speed).

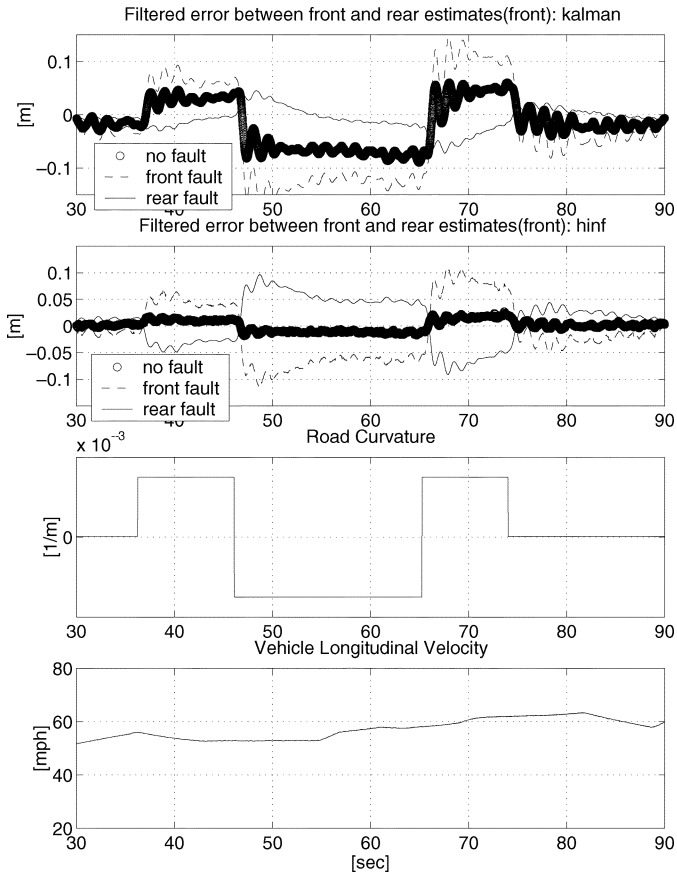

Fig. 8. Comparison of difference between estimates of dedicated observers based only on the front magnetometer measurement (filtered, high speed).

Fig. 8 shows the difference between the estimates for the high-speed emulation tests (all of the estimates are filtered by a low-pass filter). Again, we see that the fault detection performance in the case of the $\mathcal{H}_\infty$ optimized observers is observed to be better. In the case of the Kalman filter-based scheme, we cannot differentiate between the no-fault condition and the condition when the rear magnetometer fails.

VI. Summary and Conclusions

In this paper, we presented a novel approach to the design of a fault detection filter based on $\mathcal{H}_\infty$ loop-shaping methodology for the design of Luenberger observers. The choice of such a design methodology was motivated by the ease with which frequency-domain-based performance objectives can be incorporated into the design process.

The filter design problem studied in the paper pertained to the lane-keeping control system onboard vehicles used in the PATH Automated Highways program. For accurate fault detection in vehicle control systems, robustness of failure detection schemes needs special attention. The required robustness properties for the failure detection filter were translated into constraints on the frequency components of the residual signals. The aforementioned approach was applied to retune the observer gain matrices of two dedicated observes to satisfy the conditions for robustness.

Experimental results indicate that frequency shaping of residual signals helps in reducing the missed detection and false alarm rates (by maintaining the difference between the dedicated observer estimates close to zero during nonfaulty operation). We wish to mention that the success of the experiments depended significantly on the accuracy of the model used to describe the lateral dynamics of the vehicles. As mentioned earlier, the lateral dynamics of the vehicles change significantly with vehicle longitudinal velocity. Since the vehicles are operated (especially during testing) in situations where the longitudinal velocity varies over a wide range of possible values, a good gain scheduling technique, such as the linear parameter varying (LPV) technique, can potentially improve observer performance. The application of robust state estimation and filtering techniques (e.g., [24]) has also a potential to improve it.

Appendix

Here, we present the system matrices and parameters used in the design of state estimators discussed in this paper (see Table I):

$$A=\begin{bmatrix} 0 & 0 & 0 & 0 \\ 0 & -\frac{a_{11}}{\dot{x}} & a_{11} & \frac{a_{12}}{\dot{x}} \\ 0 & 0 & 0 & 1 \\ 0 & -\frac{a_{41}}{\dot{x}} & a_{41} & \frac{a_{12}}{\dot{x}} \end{bmatrix} B_1=\begin{bmatrix} 0 \\ b_{21} \\ 0 \\ b_{41} \end{bmatrix} B_2=\begin{bmatrix} 0 \\ w_{21} \\ 0 \\ w_{41} \end{bmatrix}$$

$$a_{11}=(\phi_1+\phi_2), a_{12}=\phi_1(d_s-l_f)+\phi_2(d_s+l_r),$$

$$a_{41} = \frac{l_f C_f - l_r C_r}{I_z}$$
$$a_{42} = \frac{l_1 C_f (d_s - l_f) + l_2 C_r (d_s + l_r)}{I_z}, b_{21} = \phi_1, b_{41} = \frac{l_f C_f}{I_z},$$
$$w_{21} = -\frac{l_f^2 C_f + l_r^2 C_r}{I_z}, w_{41} = \phi_2 l_r - \phi_1 l_f - \dot{x}^2$$
$$\phi_1 = C_f \left(\frac{1}{m} + \frac{l_f d_s}{I_z} \right), \phi_2 = C_r \left(\frac{1}{m} - \frac{l_r d_s}{I_z} \right)$$
$$W_{p1}(s) = \frac{9.34 \times 10^2 s^2 + 5.11 \times 10^4 s + 1.44 \times 10^6}{s^2 + 8.54 \times 10^2 s + 1.18 \times 10^6}$$
$$W_{p2}(s) = \frac{4.70 \times 10^4 s^2 + 3.46 \times 10^6 s + 2.04 \times 10^8}{s^2 + 2.01 \times 10^3 s + 3.80 \times 10^6}.$$

ACKNOWLEDGMENT

The authors would like to thank H.-S. Tan and D. Nelson of California PATH for insightful comments, suggestions, and experimental support. The contents of this paper reflect the views of the authors who are responsible for the facts and accuracy of the data presented herein. The contents do not reflect the official views or policies of the State of California.

REFERENCES

[1] P. Varaiya, "Smart cars on smart roads: Problems of control," *IEEE Trans. Autom. Control*, vol. 38, no. 2, pp. 195–207, Feb. 1993.
[2] R. Rajamani, H. S. Tan, and W. B. Zhang, "Demonstration of integrated longitudinal and lateral control for the operation of automated vehicles in platoons," *IEEE Trans. Contr. Syst. Technol.*, vol. 8, no. 4, pp. 695–708, Jul. 2000.
[3] R. Isermann, "Diagnosis methods for electronic controller vehicles," in *Proc. Plenary Lecture 5th Advanced Vehicle Control Conf.*, Ann Arbor, MI, 2000.
[4] R. Rajamani, A. Howell, C. Chen, J. K. Hedrick, and M. Tomizuka, "A complete fault diagnostic system for automated vehicles," *IEEE Trans. Contr. Syst. Technol.*, vol. 9, no. 4, pp. 553–564, Jul. 2001.
[5] K. M. Nagpal and P. P. Khargonekar, "Filtering and smoothing in the $\mathcal{H}_\infty$ setting," *IEEE Trans. Autom. Control*, vol. 36, no. 2, pp. 152–166, Feb. 1991.
[6] L. E. Ghaoui, F. Oustry, and M. AitRami, "A cone complementarity linearization algorithm for static output feedback and related problem," *IEEE Trans. Autom. Control*, vol. 42, no. 8, pp. 1171–1176, Aug. 1997.
[7] R. J. Patton, P. M. Frank, and R. N. Clark, *Fault Diagnosis in Dynamic Systems: Theory and Applications*. Upper Saddle River, N.J.: Prentice-Hall, 1989.
[8] R. Isermann, "Supervision, fault detection and fault diagnosis methods—An introduction," *Control Eng. Practice*, vol. 5, pp. 639–652, 1997.
[9] P. M. Frank, "Fault diagnosis in dynamic systems using analytical and knowledge-based redundancy—A survey and some new results," *Automatica*, vol. 26, no. 3, pp. 459–474, 1990.
[10] N. Viswanadham, J. H. Taylor, and E. C. Luce, "A frequency domain approach to failure detection and isolation with application," *Control Theory Adv. Technol.*, vol. 3, pp. 45–72, 1987.
[11] P. M. Frank and X. Ding, "Frequency domain approach to optimally robust residual generation and evaluation for model-based fault diagnosis," *Automatica*, vol. 30, no. 5, pp. 789–804, 1994.
[12] S. Suryanarayanan, M. Tomizuka, and T. Suzuki, "Fault tolerant lateral control of automated vehicles based on simultaneous stabilization," in *Proc. 1st IFAC Mechatron. Conf.*, Darmstadt, Germany, 2000, pp. 899–904.
[13] S. Suryanarayanan and M. Tomizuka, "Observer based look-ahead for fault tolerant lateral control of automated vehicles," in *Proc. 5th Int. Symp. Advanced Vehicle Control*, Ann Arbor, MI, 2000, pp. 269–274.
[14] S. Patwardhan, "Fault detection and tolerant control for lateral guidance of vehicles in automated highways," Ph.D. dissertation, Univ. California, Berkeley, 1994.
[15] J. Guldner, S. Patwardhan, and H. S. Tan, "Study of design directions for vehicle lateral control," in *Proc. 36th IEEE Conf. Decision Control*, San Diego, CA, 1996, pp. 1732–1737.
[16] I. R. Pertersen, "Disturbance attenuation and $\mathcal{H}_\infty$: A design method based on the algebraic Ricatti equation," *IEEE Trans. Autom. Control*, vol. AC-32, no. 5, pp. 427–429, May 1987.
[17] J. C. Doyle, K. Glover, P. P. Khargonekar, and B. A. Francis, "State space solutions to $\mathcal{H}_2$ and $\mathcal{H}_\infty$ control problems," *IEEE Trans. Autom. Control*, vol. 34, no. 8, pp. 544–549, Aug. 1989.
[18] S. Ibaraki and M. Tomizuka, "Tuning of a hard disk drive servo controller using fixed-structure $\mathcal{H}_\infty$ controller optimization," *Trans. ASME, J. Dyn. Syst. Meas. Control*, vol. 123, no. 3, pp. 544–549, 2001.
[19] L. Xie, C. E. de Souza, and M. Fu, "$\mathcal{H}_\infty$ estimation for discrete-time linear uncertain systems," *Int. J. Robust Nonlinear Control*, vol. 42, no. 10, pp. 111–123, 1991.
[20] H. D. Tuan, P. Apkarian, and T. Q. Nguyen, "Robust and reduced-order filtering: New characterizations and methods," in *Proc. American Control Conf.*, Chicago, IL, Jun. 2000, pp. 1327–1331.
[21] T. Song and E. G. Collins Jr., "Robust $\mathcal{H}_2$ estimation with application to robust fault detection," in *Proc. American Control Conf.*, Chicago, IL, 2000, pp. 1200–1204.
[22] W. Niu, S. Ibaraki, and M. Tomizuka, "Tuning of a disk drive servo controller using fixed-structure $\mathcal{H}_\infty$ controller optimization," *Microsyst. Technol.*, vol. 9, no. 1–2, pp. 92–98, 2002.
[23] P. Gahinet, A. Nemirovskii, A. J. Laub, and M. Chitali, "The lmi control toolbox," in *Proc. 33rd IEEE Conf. Decision Control*, Lake Buena Vista, FL, 1994, pp. 2038–2041.
[24] S. O. R. Moheimani, A. V. Savkin, and I. R. Petersen, "Robust filtering, prediction, smoothing, and observability of uncertain systems," *IEEE Trans. Circuits Syst. I, Fundam. Theory Appl.*, vol. 45, no. 4, pp. 446–457, Apr. 1998.

Soichi Ibaraki received the B.S. and M.S. degrees in precision engineering from Kyoto University, Kyoto, Japan, and the Ph.D. degree in mechanical engineering from the University of California at Berkeley.

Currently, he is a Research Associate in the Department of Precision Engineering, Kyoto University. His research interests include the application of numerical optimization to control problems, motion control of machine tools, and control and optimization issues in manufacturing systems.

Shashikanth Suryanarayanan (M'00) was born in Karaikudi, India, in 1977. He received the B.Tech degree in mechanical engineering from the Indian Institute of Technology, Madras, India, in 1998 and the Ph.D. degree in mechanical engineering from the University of California at Berkeley in 2002.

Currently, he is an Assistant Professor in the Department of Mechanical Engineering at the Indian Institute of Technology, Bombay, India. From 2003 to 2004, he was a Control Systems Engineer with the General Electric Global Research Center, Niskayuna, NY. His research interests include the application of control theory and mechatronic systems design toward the development of alternate energy devices and intelligent transportation systems.

Masayoshi Tomizuka (F'97) was born in Tokyo, Japan, in 1946. He received the B.S. and M.S. degrees in mechanical engineering from Keio University, Tokyo, Japan, and the Ph.D. degree in mechanical engineering from the Massachusetts Institute of Technology, Cambridge, in 1974.

Currently, he teaches courses in dynamic systems and controls in the Department of Mechanical Engineering, University of California at Berkeley, where he has been since 1974. He currently holds the Cheryl and John Neerhout, Jr., Distinguished Professorship Chair at the University of California at Berkeley. His current research interests are optimal and adaptive control, digital control, signal processing, motion control, and control problems related to robotics, machining, manufacturing, information storage devices, and vehicles. He has served as a consultant to various organizations, including General Electric, General Motors, and United Technologies.

Dr. Tomizuka was Technical Editor of the *ASME Journal of Dynamic Systems, Measurement and Control* (J-DSMC) from 1988 to 1993, Editor-in-Chief of the IEEE/ASME TRANSACTIONS ON MECHATRONICS from 1997 to 1999, an Associate Editor of the *Journal of the International Federation of Automatic Control*, *Automatica*, and the *European Journal of Control*. He was General Chairman of the 1995 American Control Conference, and served as President of the American Automatic Control Council from 1998—1999). He is a Fellow of the ASME and the Society of Manufacturing Engineers. He is the recipient of the Best J-DSMC Best Paper Award in 1995, the DSCD Outstanding Investigator Award in 1996, the Charles Russ Richards Memorial Award (ASME) in 1997, and the Rufus Oldenburger Medal (ASME) in 2002.